Available online at http://www.ssstj.sci.ssru.ac.th

Suan Sunandha Science and Technology Journal

Calcium Lactate as Renewable Filler of Polypropylene: Thermal, Morphological and Mechanical Properties

Buncha Suksut*, Paweena Khamsiang, Chanita Sinsawat, Nattarika Kesorn
Materials and Process Engineering Technology, Faculty of Engineering and Technology,
King Mongkut's University of Technology North Bangkok Rayong Campus, Ban Khai, Rayong 21120, Thailand
Corresponding author e-mail: * buncha.s@eat.kmutnb.ac.th

Received: *12 March 2020* / **Revised:** *11 June 2020* / **Accepted:** *7 August 2020*

Abstract

Polypropylene (PP) composites were prepared with calcium lactate (CL) at various loading levels (10-40 wt%) by melt mixing then injection molding. The resulting properties of composites were investigated by melt flow index, optical microscopy, differential scanning calorimetry, tensile, flexural and impact mechanical tests. The tensile/flexural moduli increased with increasing CL content, while the elongation at break decreased with increasing CL content. The highest tensile/flexural strengths and impact strength were found at 10 wt% CL content. The crystallization of PP initiated at higher temperature as a result of CL addition. The smaller spherulite size with the presence of CL provided the higher tie molecules, thus improving impact strength. The influence of the maleic anhydride grafted polypropylene (MAPP) as coupling agent on the properties of PP containing 10 wt% CL content was examined. The results revealed that the MAPP gave an insignificant improvement in the final properties of the composites.

Keywords: Biocomposite, Renewable filler, Calcium lactate, Polypropylene, Crystallization

1. Introduction

Nowadays, the growing environmental awareness and the concept of sustainability are the crucial factors to the use of eco-friendly materials. Therefore, the polymer-based bio-composites have been an increasing attraction to many industries (Oliver-Ortega et al., 2018). Hence, many research pay attention to the usage of petroleum-based thermoplastic filled with fillers extracted from natural and renewable resources. Because of its low cost, heat and thermal stability as well as easy processability, polypropylene (PP) is one of the most widely used thermoplastic among the petroleum-based polymers. It has application in numerous areas such as housewares, packaging, electric sectors and automobiles, etc. PP is currently combined with various bio-based renewable fillers in order to serve specific objectives or requirements, including coir, jute, kenaf, biochar, coffee grounds and sawdust, etc. (Bledzki, Franciszczak, Osman, & Elbadawi, 2015; Das, Bhattacharyya, Hui, & Lau, 2016; Essabir et al., 2018; Mir, Nafsin, Hasan, Hasan, & Hassan, 2013; Oliver-Ortega et al., 2018). However, due to difference in polarity, a poor interfacial adhesion between bio-based fillers and PP is a main drawback. This can be defeated by chemical treatment of filler or using coupling agents. Mir et al. revealed that the mechanical improvement of coir fiber filled PP composites was attributed to good interfacial adhesion between the coir fiber and PP matrix upon chemical treatment (Mir et al., 2013). A similar trend was published by Oliver-Ortega et al. (2018). They presented that the maleic anhydride grafted polypropylene (MAPP) as the coupling agent offered a strong interfacial adhesion between rapeseed sawdust and PP, that resulted in improved mechanical properties. The use of bio-based fillers provided not only the mechanical improvement, but also the crystallization ability enhancement. Das et al. (2016) reported that the presence of biochar initiated faster crystallization for PP. The biochar shifted the crystallization to higher temperature as compared to neat PP.

Calcium lactate (CL) is a calcium salt of natural lactate acid, which can be produced by lactic acid fermentation in the production of polylactic acid (PLA) (Xu & Xu, 2014). This white powder is a common source of calcium in food (Liao, Joshi, Tiwari, Park, & Kim, 2016). It has been mostly used in food industries as firming agents and food additives. Recently, CL has been introduced in several fields, including polymer industries. Because of its biocompatibility, CL has also been introduced in biomedical applications (Hwang, Kim, Joshi, & Park, 2019; Pant et al., 2013). Pant et al. (2013) revealed that the incorporation of CL improved the biomimetic mineralization of polyamide-6 nanofibers for bone compatibility. Apart from the biomimetic mineralization and biocompatibility, CL also provided the enhancement of tensile strength as presented in the polycaprolactone/CL composites (Liao et al., 2016). Sedlarik et al. (2009) also reported the improved mechanical properties of polyvinyl alcohol/CL. To the best of the authors' knowledge, there are a few literatures regarding CL-based composites. A lack of information about the morphological, thermal, and mechanical properties of CL filled PP composites, encourages authors to provide the studies to evaluate the competitiveness of this renewable material as a filler for any applications. In order to use renewable filler, there are three main objectives; the mechanical property improvement, an expensive materials matrix replacement, and non-renewable filler phase in a composite reduction (Oliver-Ortega et al., 2018). However, CL is a hydrophilic material due to its polar carboxyl group (Hwang et al., 2019). On the other hand, PP is nonpolar. The difference in polarity between PP and CL causes the immiscibility of the two materials. In order to improve the adhesion between these two materials, the addition of coupling agent is necessary. Ideally, this coupling agent should have at least two different co-monomers in its structure, where each one is compatible with each blended homopolymer to enhance the compatibility between the neat PP and the CL (Abdelwahab, Misra, & Mohanty, 2019). According to the literature, maleic anhydride grafted polypropylene (MAPP) has been used to increase the interfacial adhesion between PP and fillers (Abdelwahab et al., 2019; Bikiaris, Vassiliou, Pavlidou, & Karayannidis, 2005). The polar anhydride group in MAPP has interaction with the filler surface. This interaction leads to better adhesion and hence the increase in stress transfer between the neat PP and fillers. Therefore, theoretically, the incorporation of MAPP should result in the improved adhesion between the PP and CL and consequently enhance the mechanical properties of the PP/CL composites.

The purpose of this work is to clarify the influence of calcium lactate as filler in PP composites and to study the morphological, thermal, and mechanical properties of these composites. To this end, the effect of MAPP as the coupling agent addition is also reported. The investigation includes melt flow index measurement, optical microscopy, differential scanning calorimetry and mechanical tests (tensile, flexural and impact tests). The novelty aspect of this work can be highlighted by the fact that this is one of the first studies to involve PP matrix composites with calcium lactate.

2. Experimental

2.1 Materials

HMC Polymer provided a commercial grade polypropylene (PP) (HP553R) and calcium lactate was purchased from PURAC. The particle size and shape of CL are revealed by the high resolution SEM micrographs as presented in Figure 1. The maleic anhydride grafted polypropylene (MAPP) with average M_w of 9,100 g/mol and 8-10 wt% maleic anhydride content as coupling agent was supplied by Sigma Aldrich.

2.2 Preparation of composites

The neat PP and PP filled with various CL loadings (10-40 wt%) were first blended by melt compounding in an internal mixer (MX500, Chareon Tut) with a roller rotor speed of 60 rpm at 190°C for 20 minutes. In the selected PP/CL composite with optimal properties, MAPP was added in four different amounts, 2, 4, 6 and 8 wt%, based on the CL content. In order to get better CL particle dispersion in PP matrix, the compounds were then extruded via a co-rotating twin screw extruder (CTED22L32, Chareon Tut) with a screw speed of 60 rpm at the die temperature of 210°C. After extrusion, the extrudates were injected into a family mold (60SE, JONWAI) with a mold temperature of 40°C to produce the test specimens.

2.3 Melt flow index

Melt flow index (MFI) of neat PP and its composites was performed according to ASTM standard D1238 using melt flow indexer (MP1200, Tinius Olsen) with a weight of 2.16 kg at 230°C.

2.4 Optical properties

Thin section of 10 μm was prepared from the middle part of the injection molded specimen using manual rotary microtome (RM2235, Leica). The thin section was then immersed in oil between a glass slide and cover slip. The measurement was performed with a polarized optical microscope (DM2700M, Leica). A minimum of three sections was measured for each material.

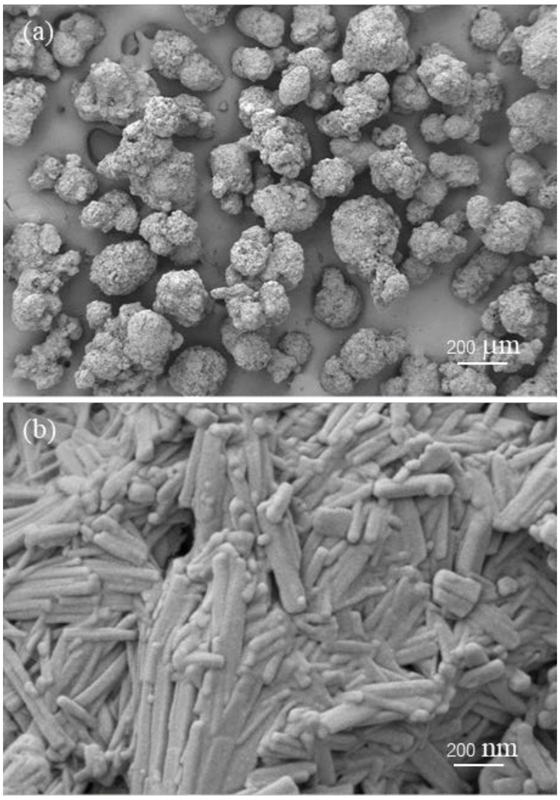

Figure 1. SEM micrographs of CL particles: (a) 50X, (b) 50000X.

2.5 Thermal properties

Thermal properties of all specimens were examined using differential scanning calorimetry (DSC, Q200, TA Instruments) equipped with the Refrigerated Cooling Systems 90 (RCS90). The samples with mass between 5 and 10 mg were placed in an aluminum pan and completely sealed with an aluminum lid. The measurements started with the heating scan with a ramp rate of 10°C/min from 0°C to 200°C and held at this temperature for 5 minutes. Then, the cooling scan was performed with a ramp rate of 10°C/min from 200°C to 0°C. The measurements were repeated for both heating and cooling scans with the same condition. The nitrogen was always purged during the measurements. The degree of crystallinity (X_C) was computed as follows:

$$X_C\,(\%) = \frac{100(\Delta H_m)/\Delta H_m^{\circ}}{\emptyset_{PP}}$$

where ΔH_m is the melting enthalpy, ΔH_m° is the theoretical heat of fusion for 100% crystalline PP (209 J/g) (Garcia et al., 2005), and $\emptyset_{PP}$ is the weight fraction of PP.

2.6 Mechanical properties

The tensile and flexural properties of the neat PP and all composites were performed using a universal testing machine (UTM, Model 25ST, Tinius Olsen). The tensile testing was measured according to ASTM standard D638 with a loading cell of 5 kN and a crosshead speed of 50 mm/min. The flexural testing was conducted according to ASTM standard D790 with a load cell of 1 kN and at a speed of 2 mm/min. According to ASTM standard D256, the notched Izod impact testing was tested using an impact tester (IT504, Tinius Olsen) with the hammer pendulum of 5.64 Jules. The 10 specimens were used for both the tensile, flexural and impact tests.

3. Results and Discussion

3.1 Effect of CL on the PP properties

Figure 2 presents the melt flow index (MFI) of PP filled with various CL loadings. The MFI is inversely proportional to the viscosity of polymer in the molten state. It is obvious that the MFI of PP composites decreases with an increase in the CL loading. The reduction in the MFI is in consequence with the rise in viscosity of the PP composites because of the restriction of molecular chain mobility imposed by the filler particles. Moreover, the presence of higher CL loading increases the possibility of the particle-particle contact and may lead to an increase in the flow resistance, thus the viscosity. This result agrees with previous studies that reported the same trend in PP and polyethylene composites (Escócio Pacheco, Silva, Cavalcante, & Visconte, 2015; Soleimani, Tabil, Panigrahi, & Opoku, 2008). The use of CL with high loading has a tendency to reduce the flowability of PP during processing, which might further limit the processability of the PP composites. However, Abdelwahab et al. (2019)

found a reduction in the MFI with the addition of coupling agent. It formed an interaction between polymer matrix and filler and helped to enhance the adhesion between the phases.

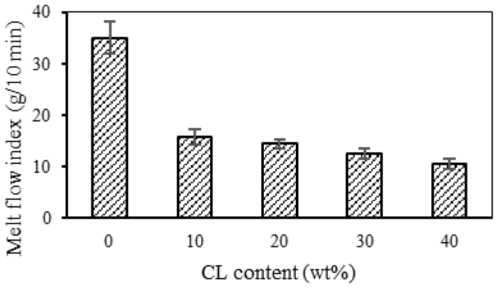

Figure 2. Melt flow index of neat PP and PP/CL composites.

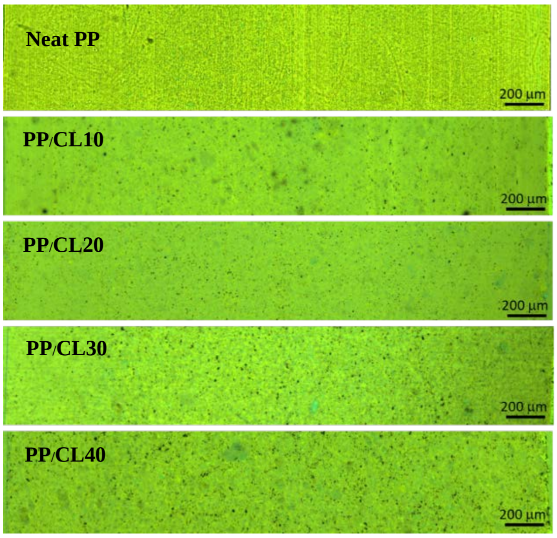

Figure 3. OM micrographs of neat PP and its composites.

Figure 3 represents the optical microscope (OM) images of materials where the CL particles (black spots) were in the PP matrix. The images were captured throughout the thickness of injection parts. These OM images reveal agglomerates of CL particles. The agglomerates become larger with increasing CL loading. This is reasonable considering that at high CL loadings, the interparticle distance become smaller, and hence the particles trend to form agglomerates.

Figure 4 reveals the spherulitic structure of neat PP and its composites. The micrographs were taken at the center of the thin section. It can be observed that the addition of CL leads to a reduction in the spherulite size, implying that CL particles or CL agglomerates act as nucleating site for PP crystallization. With the addition of CL, the higher density of nuclei provides the smaller spherulite size. However, at higher loading the agglomeration of CL particle is found, therefore the larger spherulite can be observed. A similar observation was reported by Palza et al. in PP/silica nanocomposites (Palza, Vera, Wilhelm, & Zapata, 2011).

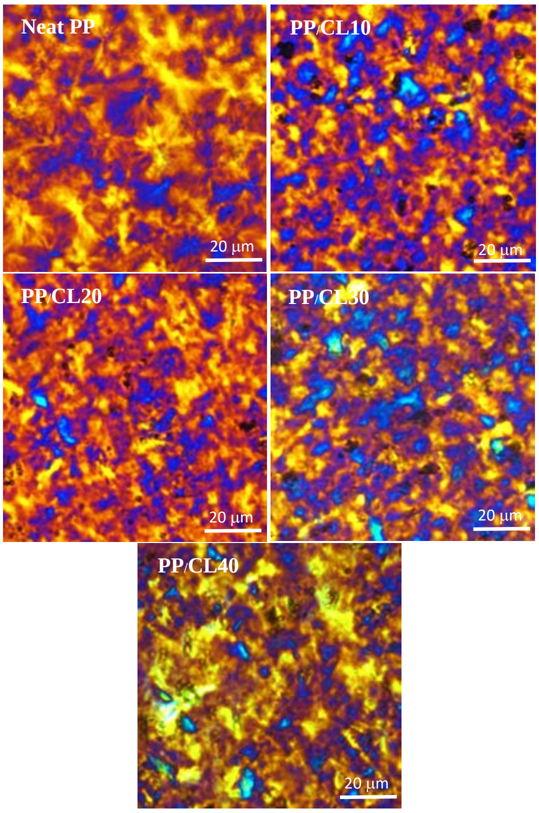

Figure 4. Spherulitic structure of neat PP and PP/CL composites.

The DSC thermograms of the second heating and cooling scans of neat PP and PP/CL composites are presented in Figure 5 and all DSC parameters are summarized in Table 1. A single peak at about 162°C during the second heating is attributed to the melting of α-crystal of neat PP (Padden & Keith, 1959). However, the T_m of PP remains almost constant in all composites. According to Table 1, the difference in the T_c of PP in all composites is significant compared to neat PP. The incorporation of CL increases the T_c of PP. The increase in T_c with increasing CL loading is also observed. The higher crystallization peak would suggest a faster crystallization in the PP/CL composites in comparison with neat PP. This is a result of the CL particle acting as a heterogeneous nucleation site. The existence of foreign particle in the polymer melt reduces the energy needed to form a new surface and also reduces the nucleus size for crystal growth (Mucha, and Królikowski, 2003). This provides the faster nucleation rate, thus the overall crystallization rate.

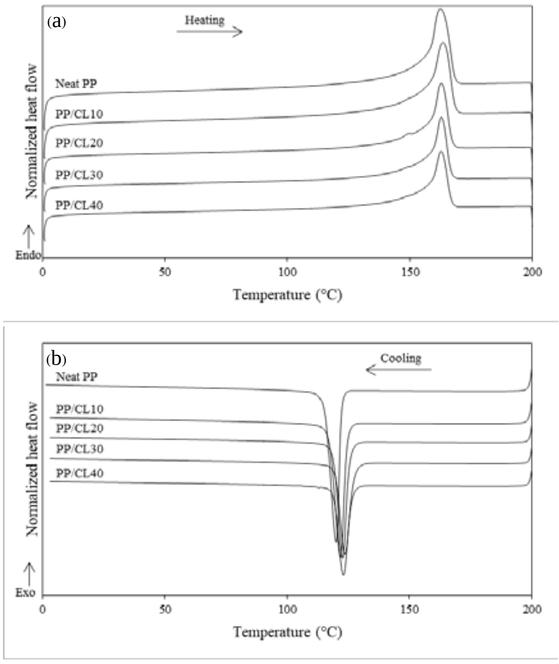

Figure 5. DSC thermograms of neat PP and its composites during (a) second heating and (b) cooling scans.

The degree of crystallinity (X_c) of neat PP was evaluated as 43.4%. It is obvious that the CL inclusion affects the X_c of PP as listed in Table 1. The X_c decreases with increasing CL loading. The addition of 10 wt%, 20 wt%, 30 wt% and 40 wt% CL to PP decreases the X_c considerably to 35.5%, 32.9%, 24.9% and 19.4%, respectively. The decrease in the X_c of PP is due to CL particles inhibiting the PP segment mobility and disrupting the PP chain structure regularity (Abdelwahab et al., 2019).

Table 1. DCS parameters of neat PP and CL filled PP composites.

Materials	T_c (°C)	T_m (°C)	ΔH_m (J/g)	X_m (%)
Neat PP	120.0	162.3	90.7	43.4
PP/CL10	121.9	163.6	82.4	35.5
PP/CL20	122.8	162.8	85.9	32.9
PP/CL30	123.8	162.9	74.4	24.9
PP/CL40	123.0	162.8	67.4	19.4

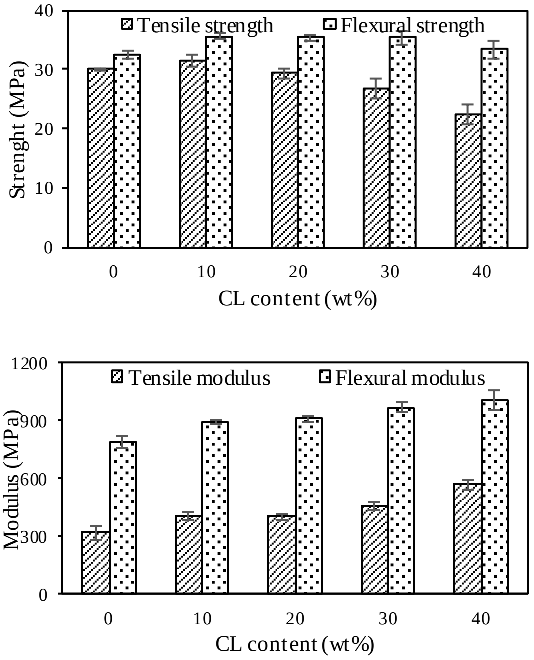

Figure 6. Mechanical properties of neat PP and CL filled PP composites (a) tensile and flexural strengths (b) tensile and flexural modulus.

Figure 6 illustrates the tensile and flexural properties of PP and its composites. It can be seen that the tensile and flexural strengths of PP increase with the incorporation of 10 wt% of CL. However, with further increase in the CL loading beyond 10 wt%, tensile and flexural strengths linearly decrease with the CL loading. At the higher filler loading, the distance between neighbor particles becomes smaller and tends to agglomerate (Altay et al., 2019), as observed in OM micrographs. Moreover, the difference in the polarity between PP matrix and CL leads to poor adhesion and hence the reduction in transfer stress between the neat PP and CL particles.

It can also be noticed from Figure 3 that the tensile and flexural moduli increase with the addition of CL. The moduli of PP increase with increasing CL loading. This is because of the higher modulus of filler particles (Altay et al., 2019). The increases in the modulus with filler loading is in accordance with other reported research (Das et al., 2016; Essabir et al., 2018; Mir et al., 2013).

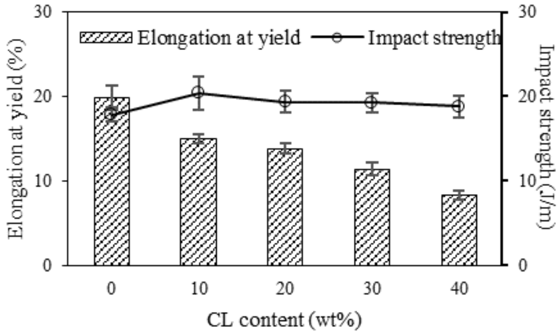

Figure 7. Elongation at break and impact strength of neat PP and PP/CL composites.

In the case of elongation at break, the results are as expected. The incorporation of CL causes a huge decrease in the elongation at break of PP as illustrated in Figure 7. Since the CL particles are rigid and have no elongation, they restrict the polymer molecules flowing past one another. It also seems that the reduction in the elongation of PP is a function of CL loading. As mentioned earlier, the formation of CL agglomeration can occur at higher CL loading. This agglomeration can act as stress concentration and breaking point of the composites (Bikiaris et al., 2005).

The notched Izod impact strength of neat PP and its composites is presented in Figure 6. It is clear that the impact strengths of the PP/CL composites are higher than that of neat PP. The smaller spherulite size of PP/CL composites may be responsible for the improvement of impact strength. The smaller spherulite size always accompanies the higher tie-molecules, improving the molecular entanglement between crystals lamellae. Thus, it leads to an increase of impact strength (Xu, Yu, & Jin, 2001). In addition, the impact strength of PP is independent of CL loading. Based on the tensile, flexural and impact properties of PP, the optimum loading of CL is 10 wt%. This composition was chosen for the study of the influence of the coupling agent addition in the following section.

3.2 Effect of MAPP on the PP/CL composite properties

The effect of MAPP on the MFI of PP composites is shown in Figure 8. MAPP slightly increases the MFI of the composites when compared with composite without coupling agent. An increase in the MFI is in consequence with the decrease in the viscosity of PP composites. There are two possible explanations for this phenomena. The first one is that MAPP acts as an internal lubricant to aid the PP chain motion. The MAPP may help to enhance the intermolecular free volume between polymer chains, thus reducing the polymer viscosity (Poletto, 2018). The second reason may be associated with the migration of the MAPP toward the composite surface. This forms a slip in the composite layers to the die, resulting in an increase in the MFI (Poletto, 2018).

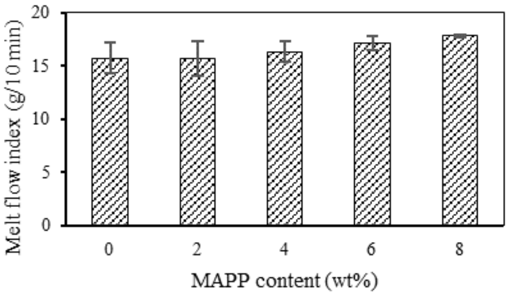

Figure 8. Melt flow index of PP composites filled with MA.

For effective improvement of mechanical properties, strong interfacial adhesion between PP and CL particles is necessary. Although an enhancement in the tensile strength and modulus of PP is expected due to better adhesion between PP matrix and CL particles using MAPP, this however, is not the case. Concerning the effect of the addition of MAPP, it appears that it has a negative effect on both the tensile strength and the modulus as presented in Figure 9 (a). The addition of MAPP coupling agent exhibits a small decrease on both tensile properties of PP. The results of elongation at break are shown in Figure 9 (b). An increase of elongation at break can be observed with addition of MAPP. The maximum elongation is at the MAPP loading of 6 wt%. It also can be observed from the Figure 9 (b) that the impact strength of PP/CL composites are independent of MAPP content. These unexpected results may be caused by several factors: (i) the deterioration of MAPP during the processing, (ii) no interaction between MAPP as the MAPP migrate to the composite surface and CL, (iii) MAPP act as lubricant for PP composites.

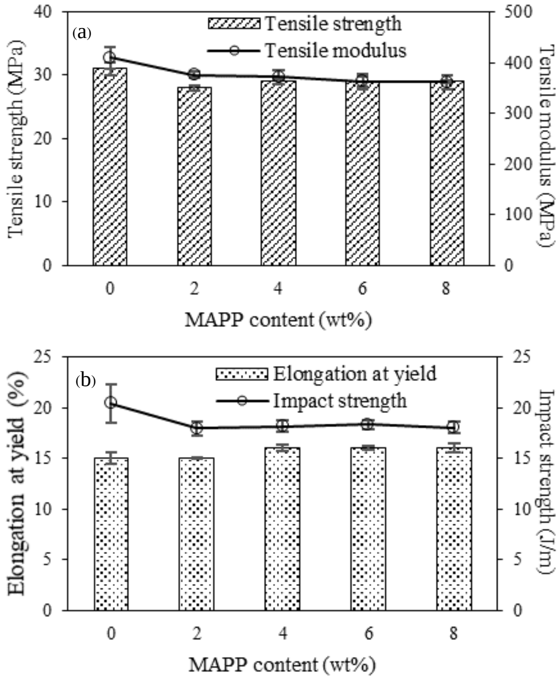

Figure 9. Mechanical properties of PP/CL composites with addition of MAPP (a) tensile strength and modulus (b) elongation at break and impact strength.

4. Conclusion

This work aimed to study the effect of calcium lactate addition in PP composites. PP composites were prepared with different amount of calcium lactate (0, 10, 20, 30, and 40 wt%) using melt mixing and injection molding. Morphological, thermal, and mechanical properties of the PP/calcium lactate composites were characterized. The addition of increasing calcium lactate content (up to 40 wt%) to neat PP continuously enhanced the tensile/flexural moduli of the composites. The maximum value of the tensile/flexural strengths and impact strength were found at 40 wt% calcium lactate loading. However, when neat PP was added with calcium lactate, a decrease in elongation at break was found in the composites. Furthermore, the presence of calcium lactate provided the smaller spherulite size, faster crystallization initiation, but lower degree of crystallinity as compared to neat PP. It can be drawn from the investigation that the resulting properties of the composites was a result of a competition effect between the interfacial adhesion of two phases and the morphological structure of the composites. In addition, the use of coupling agent offered insignificant mechanical improvements in this work.

5. Acknowledgements

The authors gratefully acknowledge HMC Polymer for the supply of polypropylene. The authors also thank the faculty of Engineering and Technology, King Mongkut's University of Technology North Bangkok Rayong Campus for supporting the project.

6. Publication Ethic

Submitted manuscripts not have been previously published by or be under review by another print or online journal or source.

7. References

Abdelwahab, M. A., Misra, M., & Mohanty, A. K. (2019). Injection molded biocomposites from polypropylene and lignin: Effect of compatibilizers on interfacial adhesion and performance. *Industrial Crops and Products, 132,* 497-510. doi: 10.1016/j.indcrop.2019.02.026

Altay, L., Atagur, M., Sever, K., Sen, I., Uysalman, T., Seki, Y., & Sarikanat, M. (2019). Synergistic effects of graphene nanoplatelets in thermally conductive synthetic graphite filled polypropylene composite. *Polymer Composites, 40*(1), 277-287. doi:10.1002/pc.24643

Bikiaris, D. N., Vassiliou, A., Pavlidou, E., & Karayannidis, G. P. (2005). Compatibilisation effect of PP-g-MA copolymer on iPP/SiO_2 nanocomposites prepared by melt mixing. *European Polymer Journal, 41*, 1965-1978. doi:10.1016/j.eurpolymj.2005.03.008

Bledzki, A. K., Franciszczak, P., Osman, Z., & Elbadawi, M. (2015). Polypropylene biocomposites reinforced with softwood, abaca, jute, and kenaf fibers. *Industrial Crops and Products, 70,* 91-99. doi:10.1016/j.indcrop.2015.03.013

Das, O., Bhattacharyya, D., Hui, D., & Lau, K.-T. (2016). Mechanical and flammability characterisations of biochar/polypropylene biocomposites. *Composites Part B, 106*, 120-128. doi:10.1016/j.compositesb.2016.09.020

Escócio, V. A., Pacheco, E. B. A. V., Silva, A. L. N., Cavalcante, A. P., & Visconte, L. L. Y. (2015). Rheological behavior of renewable polyethylene (HDPE) composites and sponge gourd (*Luffa cylindrica*) residue. *International Journal of Polymer Science, 2015*. doi:10.1155/2015/714352

Essabir, H., Raji, M., Laaziz, S. A., Rodrique, D., Bouhfid, R., & Qaiss, A. E. K. (2018). Thermo-mechanical performances of polypropylene biocomposites based on untreated, treated and compatibilized spent coffee grounds. *Composites Part B, 149*, 1-11. doi:10.1016/j.compositesb.2018.05.020

Garcia, M., van Vliet, G., Jain, S. , Schrauwen, B. A. G., Sarkissov, A., van Zyl, W. E., & Boukamp, B. A. (2005). Polypropylene/SiO_2 nanocomposites with improved mechanical properties. *Reviews on Advanced Materials Science*, *6*(2), 169-175.

Hwang, T. I., Kim, J. I., Joshi, M. K., & Park, C. H. (2019). Simultaneous regeneration of calcium lactate and cellulose into PCL nanofiber for biomedical application. *Carbohydrate Polymers*, *212*, 21-29. doi:10.1016/j.carbpol.2019.01.085

Liao, N., Joshi, M. K., Tiwari, A. P., Park, C. H., & Kim, C. S. (2016). Fabrication, characterization and biomedical application of two-nozzle electrospun polycaprolactone/zein-calcium lactate composite nonwoven mat. *Journal of the Mechanical Behavior of Biomedical Materials, 60*, 312-323. doi:10.1016/j.jmbbm.2016.02.006

Mir, S. S., Nafsin, N., Hasan, M., Hasan, N., & Hassan, A. (2013). Improvement of physico-mechanical properties of coir-polypropylene biocomposites by fiber chemical treatment. *Materials and Design*, *52*, 251-257. doi:10.1016/j.matdes.2013.05.062

Mucha, M. & Krolikowski, Z. J. (2003). Application of DSC to study crystallization kinetics of polypropylene containing fillers. Journal of Thermal Analysis and Calorimetry , 74(2),549-557. doi.org/10.1023/B:JTAN.0000005193.66789.ea

Oliver-Ortega, H., Chamorro-Trenado, M. A., Soler, J., Mutjé, P., Vilaseca, F., & Espinach, F. X. (2018). Macro and micromechanical preliminary assessment of the tensile strength of particulate rapeseed sawdust reinforced polypropylene copolymer biocomposites for its use as building material. *Construction and Building Materials, 168,* 422-430. doi:10.1016/j.conbuildmat.2018.02.158

Padden, F. J., & Keith, H. D. (1959). Spherulitic crystallization in polypropylene. *Journal of Applied Physics*, *30*, 1479. doi:10.1063/1.1734985

Palza, H., Vera, J., Wilhelm, M., & Zapata, P. (2011). Spherulite growth rate in polypropylene/silica nanoparticle composites: Effect of particle morphology and compatibilizer. *Macromolecular Materials and Engineering*, *296*(8), 744-751. doi:10.1002/mame.201000405

Pant, H. R., Risal, P., Park, C. H., Tijing, L. D., Jeong, Y. J., & Kim, C. S. (2013). Synthesis, characterization, and mineralization of polyamide-6/calcium lactate composite nanofibers for bone tissue engineering. *Colloids and Surfaces B: Biointerfaces*, *102*, 152-157. doi:10.1016/j.colsurfb.2012.08.032

Poletto, M. (2018). Influence of coupling agents on rheological, thermal expansion and morphological properties of recycled polypropylene wood flour composites. *Maderas: Ciencia y Tecnología*, *20*(4), 563-570. doi:10.4067/S0718-221X2018005004401

Sedlarik, V., Galya, T., Emri, I., & Saha, P. (2009). Structure and conditioning effect on mechanical behavior of poly (vinyl alcohol)/calcium lactate biocomposites. *Polymer Composites*, *30*(8), 1158-1165. doi:10.1002/pc.20672

Soleimani, M., Tabil, L., Panigrahi, S., & Opoku, A. (2008). The effect of fiber pretreatment and compatibilizer on mechanical and physical properties of flax fiber-polypropylene composites. *Journal of Polymers and the Environment*, *16*, 74-82. doi:10.1007/s10924-008-0102-y

Xu, K., & Xu, P. (2014). Efficient calcium lactate production by fermentation coupled with crystallization-based in situ product removal. *Bioresource Technology*, *163*, 33-39. doi:10.1016/j.biortech.2014.04.002

Xu, T., Yu, J., & Jin, Z. (2001). Effects of crystalline morphology on the impact behavior of polypropylene. *Materials and Design, 22,* 27-31. doi:10.1016/S0261-3069(00)00033-9